Algorithms for the Analysis and Processing of Autostereoscopic Images

Efthymios T. Koufogiannis*

Department of Informatics and Telecommunications
National and Kapodistrian University of Athens
efthimis@di.uoa.gr

Abstract. Nowadays, acquisition and display of three-dimensional (3D) images requires the use of special tracking devices or glasses. However specialized techniques provide the ability of 3D content delivery to end users without such limitations. These methods are called autostereoscopic and the resulting images are called autostereoscopic images.
A promising type of autostereoscopic imaging is called Integral Imaging (InI). InI provides the ability of capturing Integral Images (InIms) that contain embedded 3D information and are additionally able to display it to the end user without the need for specialized equipment. But the existence of even slight misalignments between the optical components in the acquisition device results in geometrical aberrations in the structure of the acquired InIm. These result in total loss of the displayed 3D content as well as failure of all InI analysis and processing algorithms that depend on predetermined geometric dimensions of the acquired InIm. In this doctoral dissertation robust image processing frameworks were developed in order to successfully correct these geometrical aberrations.
In detail, using computer vision methodologies, the problems of geometrical aberrations in arrays of square, hexagonal-triangular as well as circular lenses were extensively studied, a process that resulted in the development of robust InIm processing and rectification algorithms.

Keywords: Three dimensional image, Autostereoscopic image, Integral photography, Computer vision, Projective distortion

1 Introduction

Current technological developments in sensor and display technologies as well as in the manufacturing of optical components have made possible the creation of novel three-dimensional (3D) capturing as well as display devices. These devices are currently penetrating consumer market applications, therefore there is a need for improving them and increasing their robustness. This doctoral dissertation focuses on images acquired from Integral Imaging (InI), systems. The InI principle which was initially formulated by the Nobel laureate G. Lippman

* Dissertation Advisor: Manolis Sangriotis, Associate Professor.

[1] back in 1908, is currently considered as one of the most promising techniques for delivering 3D content, featuring full color, adequate detail and depth levels as well as support for multiple simultaneous viewers [2].

The basic InI acquisition setup shown in Fig. 1(a) consists of a charged coupled device (CCD) and a lens array (LA) that projects a real world scene on the CCD, forming a number of Elemental Images (EIs) depicting different parts of the acquired scene. The corresponding display setup shown in Fig. 1(b)

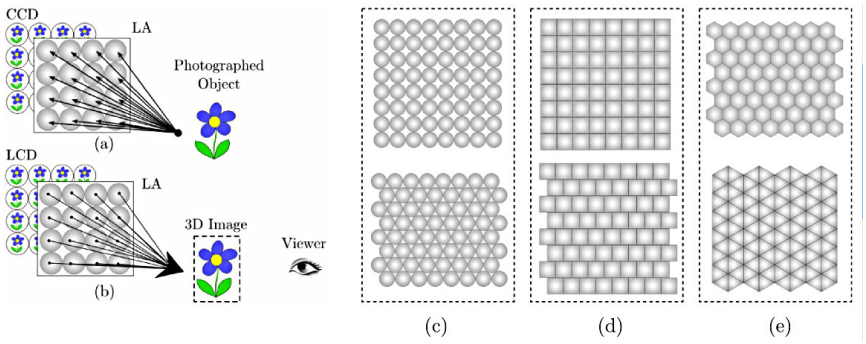

Fig. 1. (a) Integral Imaging acquisition, (b) InI display setup, (c), (d), (e) arrays of circular, square and hexagonal-triangular lenses.

reverses the previous procedure by using a liquid crystal display (LCD) between the image formed on the CCD and the LA. This results in a 3D image being projected between the LA and the viewer. It should be noted that LAs come in different configurations containing circular, round, and hexagonal-triangular lenses as shown in Figs. 1(c), 1(d), 1(e). Additional details of the InI display and acquisition processes can be found in [3], [4].

Since misalignments almost always occur during the InIm acquisition stage, perspective distortion is introduced which alters the expected shape of the resulting EIs. This results in degrading the resulting EI grid since the acquired EIs do not have constant geometric properties and are not properly aligned and sized. The result is total loss of the 3D information on the display setup. Furthermore all subsequent InI processing tasks such as compression [5] and 3D object reconstruction [6] fail since they depend on the accurate location as well as dimension of the acquired EIs.

Previous work on this field initially [7] focused on slight rotational and translational misalignments between the CCD and arrays of square lenses during the InI acquisition phase. In [8] an initial approach to the problem of perspective distortion on square lens setups was proposed where a single rectangle detected using the Hough Transform inside the area of a distorted InIm was used to extract the necessary rectification parameters.

2 Dissertation Summary

In this doctoral dissertation efficient and robust image analysis and processing algorithms were proposed in order to rectify geometric distortions not only for InIms acquired using arrays of square lenses, but for all commonly used lens array configurations.

Using computer vision methodologies geometric distortions corresponding to InIms acquired using arrays of square [9], hexagonal-triangular [10] and circular [11], [12] lenses were corrected by utilizing statistical image wide features. Furthermore the rectification process for square, hexagonal and triangular lens arrays was further streamlined by using a least squares approach that led to a simple and efficient implementation that bypassed all intermediate matrix computations.

It should be noted that in this thesis and for the first time in current literature, an effective approach was suggested in order to alleviate geometric distortions occurring from arrays of circular lenses. Circular lenses are still widely used in existing setups [13] and in this work effective algorithms where implemented both for rotational [11] as well as perspective distortion [12] in arrays of circular lenses regardless of lens packing configuration.

3 Perspective Rectification

According to [14] the transformation corresponding to perspective distortion is mathematically represented by the 3×3 real value matrix H^{-1}. The inverse procedure results in the perspective rectification matrix H that maps a point $\mathbf{x}$ from the distorted image to its corresponding point $\mathbf{x}'$ on the rectified image using

$$\mathbf{x}' = H\mathbf{x} \tag{1}$$

where $\mathbf{x}$ and $\mathbf{x}'$ are three-vectors in homogeneous coordinates representing the relevant points on the two-dimensional (2D) projective space. In a similarly way distorted lines on the 2D projective space are rectified using H^{-T} [14]:

$$\mathbf{l}' = H^{-T}\mathbf{l} \tag{2}$$

Furthermore and according to Liebowitz [15] the perspective transformation H can be stratified as a breakdown structure that consists of the three matrices H_p, H_a, H_s:

$$H = H_s H_a H_p \tag{3}$$

where

$$H_p = \begin{bmatrix} 1 & 0 & 0 \\ 0 & 1 & 0 \\ l_1 & l_2 & l_3 \end{bmatrix} \tag{4}$$

$$H_a = \begin{bmatrix} \frac{1}{\beta} & \frac{-\alpha}{\beta} & 0 \\ 0 & 1 & 0 \\ l_1 & l_2 & l_3 \end{bmatrix} \tag{5}$$

$$H_s = \begin{bmatrix} sR & \mathbf{t} \\ \mathbf{0}^T & 1 \end{bmatrix} \tag{6}$$

This stratified rectification approach and its results from the subsequent application of H_p, H_a, H_s is demonstrated in Fig. 2 for a perspectively distorted checkerboard image.

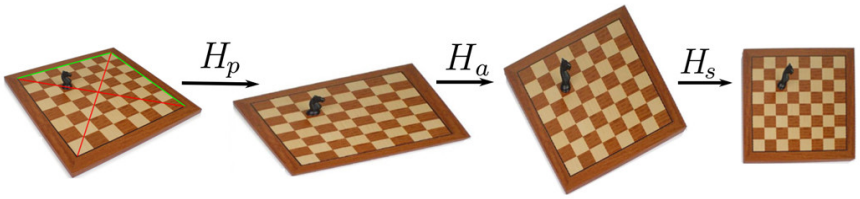

Fig. 2. Subsequent application of the matrices H_p, H_a and H_s results in a perspectively rectified image.

More analytically, matrix H_p consists of the parameters l_1, l_2, l_3. These parameters define the vanishing line (horizon line) $l_1x+l_2y+l_3 = 0$ of the distorted image plane. As seen in the second image of Fig. 2 applying H_p removes the projective component of the distortion resulting in an image where line parallelism has been restored but length and angle ratios are wrong.

Matrix H_a consists of the parameters α, β that restore the metric properties on the affine image. These parameters are calculated by measuring foreknown geometric properties such as length and line ratios on the affine image and subsequently applying the metric constraints described in [15]. Application of H_a results in an arbitrarily rotated and scaled image with correct metric properties as seen in the third image of Fig. 2.

Finally applying H_s results in correct rotation and scaling as seen in the rightmost image of Fig. 2. It should be noted that R is a rotational matrix, s is a scaling parameter while $\mathbf{t}$ is a translation vector.

3.1 Least Squares based Rectification

For our specific InIm rectification purposes translation and scaling in the final stage of the rectification procedure are not needed since they can be calculated during the InI display stage. Therefore the perpective rectification matrix H will have six degrees of freedom and the form of

$$H = \begin{pmatrix} h_1 & h_2 & 0 \\ h_3 & h_4 & 0 \\ h_5 & h_6 & 1 \end{pmatrix} \tag{7}$$

According to Eq. 2 the corresponding line transformation matrix has the form H^{-T} and is given by

$$H_L = (H^{-1})^T = \begin{pmatrix} g_1 & g_3 & g_5 \\ g_2 & g_4 & g_6 \\ 0 & 0 & 1 \end{pmatrix} \tag{8}$$

In the case of a hexagonal-triangular EI grid and by using the foreknown ideal line angles of 90°, −30°, 30° the line rectification matrix can be estimated by forming a Homogeneous Overdetermined Linear System (HOLS) using only the distorted line parameters $\{\mathbf{d}, \mathbf{b}\}$ as seen in Eq. 9.

$$\begin{pmatrix} \mathbf{0}^T & \mathbf{d}_{v1}^T \\ \mathbf{0}^T & \mathbf{d}_{v2}^T \\ \vdots & \vdots \\ \mathbf{0}^T & \mathbf{d}_{vN_v}^T \\ \mathbf{d}_{a1}^T & \lambda \mathbf{d}_{a1}^T \\ \mathbf{d}_{a2}^T & \lambda \mathbf{d}_{a2}^T \\ \vdots & \vdots \\ \mathbf{d}_{aN_a}^T & \lambda \mathbf{d}_{aN_a}^T \\ \mathbf{d}_{b1}^T & -\lambda \mathbf{d}_{b1}^T \\ \mathbf{d}_{b2}^T & -\lambda \mathbf{b}_{a2}^T \\ \vdots & \vdots \\ \mathbf{d}_{bN_b}^T & -\lambda \mathbf{b}_{bN_b}^T \end{pmatrix} \begin{pmatrix} g_1 \\ g_3 \\ g_5 \\ g_2 \\ g_4 \\ g_6 \end{pmatrix} = \mathbf{0} \tag{9}$$

On the previous system, $\lambda = \sqrt{3}/3$, $\mathbf{0}^T = [0, 0, 0]$ and $\mathbf{0}$ is column vector containing as many zeros as the total number of distorted lines detected. The least squares solution of the previous system results in the estimation of the parameters $g_1, g_2, \ldots, g_6$.

3.2 Rectification of InIms acquired from Arrays of Circular Lenses

An initial approach to geometric distortion of InIms acquired from arrays of circular lenses was proposed in [11] where the problem of InIm rotation was resolved using the Gradient augmented Circular Hough Transform [16] and a subsequent Delaunay triangulation on the centers of the resulting centers in order to identify the rotation angle.

But in the case of perspective distortion the imaged EIs are being mapped to elliptical shapes. Therefore all available line or circle detection methods are of no use since the only available structures found inside the distorted InIms are elliptical contours. In this case a different mathematical approach is applied to calculate the necessary rectification matrices H_p, H_a, H_s.

This approach is based on the theory of the Circular Points [14] that are the two complex conjugate three-vectors $(1, \pm i, 0)^T$ located at the infinity on the undistorted InIm plane. All coplanar circles verify their coordinates [17], [18].

The corresponding Images of the Circular Points are the conjugate three-vectors $(\alpha l_3 \mp i l_3 \beta, l_3, -l_2 - l_1 \alpha \pm i l_1 \beta)^T$ that are located on the vanishing line of the distorted InIm plane after the perspective distortion H^{-1} has occured. All coplanar ellipses on the distorted plane verify their coordinates.

Obtaining the coordinates $(x_c, y_c, 1)^T$ and $(\overline{x_c}, \overline{y_c}, 1)^T$ for the two conjugate ICPs results in the extraction of all necessary rectification parameters in the matrices H_p, H_a, H_s as shown in Fig. 3.

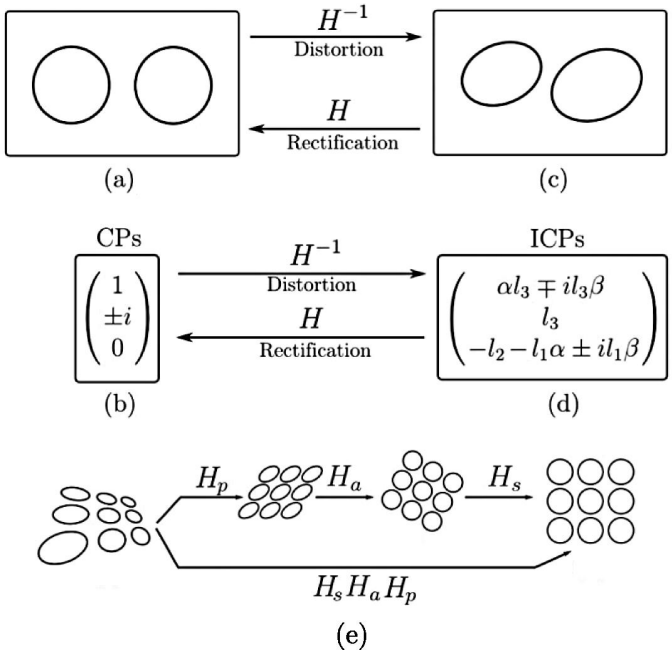

Fig. 3. (a) Any pair of coplanar circles verifies the CPs shown in (b). Under the perspective distortion H^{-1}, the pair of ellipses in (c) corresponding to the circles in (a) verifies the ICPs shown in (d). (e) Subsequent application of the matrices H_p, H_a and H_s results in a perspectively rectified image.

These parameters are given by

$$(l_1, l_2, l_3)^T = (x_c, y_c, 1)^T \times (\overline{x_c}, \overline{y_c}, 1)^T \tag{10}$$

$$\begin{cases} \alpha = \text{Real}\left(\frac{-l_2 x_c}{l_3 + l_1 x_c}\right) = \text{Real}\left(\frac{l_3 + l_2 y_c}{-l_1 y_c}\right) \\ \beta = \left|\text{Imag}\left(\frac{-l_2 x_c}{l_3 + l_1 x_c}\right)\right| = \left|\text{Imag}\left(\frac{l_3 + l_2 y_c}{-l_1 y_c}\right)\right| \end{cases} \tag{11}$$

A fully detailed methodology containing all the necessary steps followed to extract the ICPs as well as the corresponding rectification parameters $l_1, l_2, l_3, \alpha, \beta$ in a real case distorted InIm scenario is seen in [12].

4 Line Segment Detection and Clustering

In order to efficiently detect line segments corresponding to EI border edges for arrays of square and hexagonal lenses we used the LSD algorithm [19] which is robust against noise, minimizes the number of false segment detections and has linear execution time.

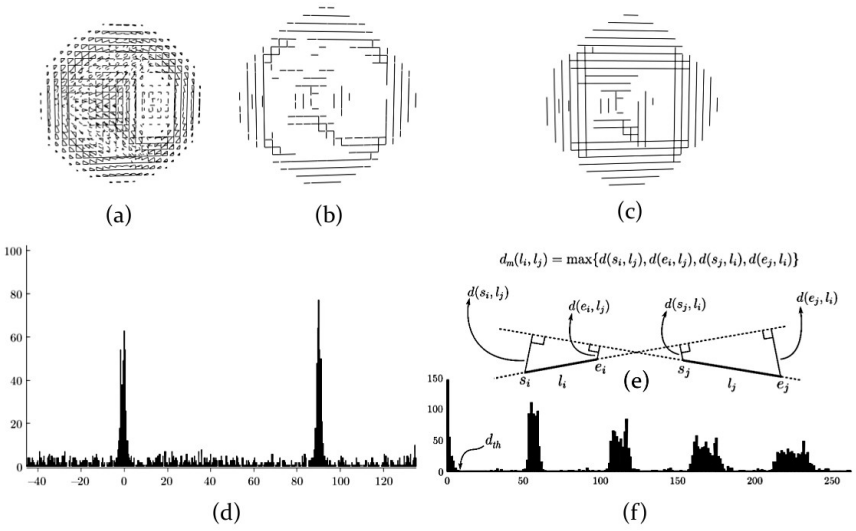

Fig. 4. (a) Acquired InIm after applying the LSD algorithm. (b) Segments resulting after isolating the histogram lobes shown in (d). (c) Clustering of line segments from (b) after using the clustering function of (e) and using its histogram in (f).

Application of the LSD on an acquired InIm results in the EI segments shown in Fig 4(a). Further calculation of the segment angles and isolation of the segments corresponding to the main lobes of the angles histogram results in a significant reduction of the noisy segments as shown in Fig 4(b).

Finally a hierarchical clustering [20] approach using a custom metric function operating between segments and a subsequent least squares fitting of the line segments in the resulting clusters results in very accurate lines corresponding to EI borders as shown in Fig 4(c). For a more concrete analysis of this line isolation framework the reader can refer to [9].

5 Elliptical Contour Extraction

To efficiently estimate analytical equations of ellipses corresponding to distorted EI borders an edge linking [21] approach was applied followed by elliptical fitting using a least squares approach. The best 20% of the fitting results (according

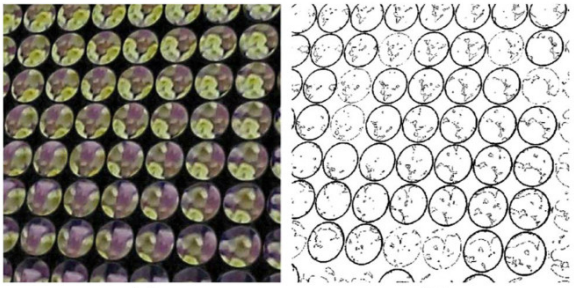

(a) (b)

Fig. 5. (a) Perspectively distorted InIm acquired using an array of circular lenses. (b) Elliptical contours extracted after applying an edge linking and ellipse fitting approach.

to their Mean Squared Error) were retained in order to obtain accurate elliptical borders. This approach is demonstrated in Fig 5 and for all the relevant implementation details the reader may refer to [12].

6 Experimental Results and Discussion

A large number of different artificially generated InIms featuring different types of LAs, varying levels of texture details and object complexity were generated using the methodology proposed in [22]. In Fig. 6 an artificial "Teapot" has been rendered using an array of square lenses while in Fig. 8 a "3D Objects" scene has been rendered using an array of circular lenses.

Furthermore to effectively assess the robustness of our InIm analysis and rectifications algorithms, the computer generated images were contaminated with Gaussian noise resulting in image qualities of 30, 25 and 20 dB. Following this approach provided full control over the introduced perspective distortion as well as prior knowledge of the ground truth values for the rectification parameters.

In addition to the computer generated images a large number of optically acquired InIms was acquired featuring different scene complexities, utilizing arrays of square, hexagonal as well as circular lenses. Figure 7 features an optically acquired "Dice" using an array of square lenses, while Fig. 9 features an optically acquired "Toy" using an array of circular lenses.

We used two geometric consistency metrics that statistically characterize the consistency of the rectified InIm grid after applying the rectification methodologies proposed in this dissertation. For square lens packing configurations we used the fact that the reconstructed grid separating the lenses is characterized by equally spaced intersecting lines forming angles of 90°. To evaluate the deviations from an ideal grid we calculated the angles $\{\omega\}$ as well as the segment lengths $\{\lambda\}$ formed between the intersecting lines of the grid. We used a similar approach for arrays of hexagonal lenses [10] by considering line angle values of $-30°$, $30°$ and $90°$.

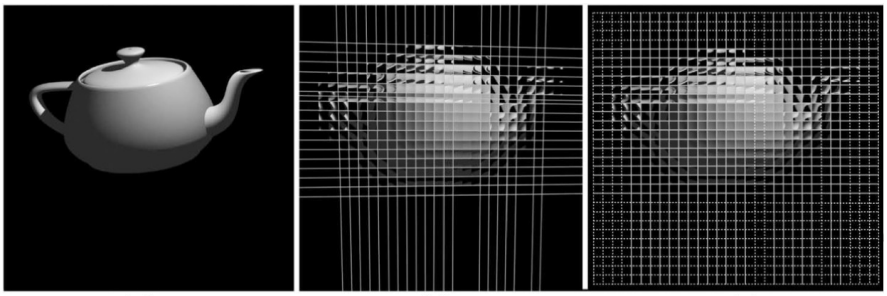

(a) (b) (c)

	$\bar{\omega}_i \pm \sigma_{\omega_i}$	$\bar{\lambda}_i \pm \sigma_{\lambda_i}$
noiseless	$90.000° \pm 0.060°$	0.996 ± 0.011
30 dB	$90.00° \pm 0.10°$	1.009 ± 0.013
25 dB	$90.00° \pm 0.12°$	1.009 ± 0.017
20 dB	$90.00° \pm 0.16°$	0.999 ± 0.024

(d)

Fig. 6. Rectification results for a representative artificially generated InIm. (a) The original 2D image of a 3D "Teapot", (b) the corresponding perspectively distorted InIm, (c) the rectified InIm along with the registered grid lines superimposed, (d) the corresponding geometric consistency parameter values for various noise levels.

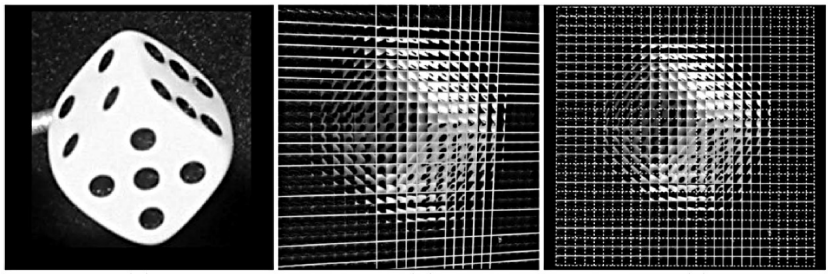

(a) (b) (c)

$\bar{\omega}_i \pm \sigma_{\omega_i}$	$\bar{\lambda}_i \pm \sigma_{\lambda_i}$
$90.000° \pm 0.055°$	1.006 ± 0.010

(d)

Fig. 7. Rectification results for an optically acquired InIm. (a) The original 2D acquired image of a real "Dice", (b) the corresponding perspectively distorted InIm, (c) the rectified InIm along with the registered grid lines superimposed, (d) the corresponding geometric consistency parameter values.

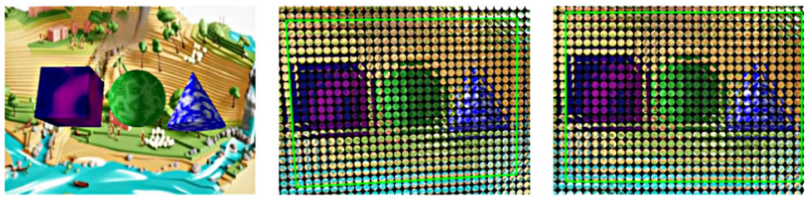

(a) (b) (c)

	$\overline{\omega_i} + \sigma_{\omega_i}$	σ_{λ_i}
Noiseless (dB)	$90.00 \pm 0.15°$	0.014
30	$90.00 \pm 0.17°$	0.022
25	$90.00 \pm 0.52°$	0.037
20	$90.00 \pm 0.87°$	0.041

(d)

Fig. 8. Rectification results for a representative artificially generated InIm acquired using an array of circular lenses. (a) The original 2D image of the "3D Objects", (b) the corresponding perspectively distorted InIm, (c) the rectified InIm, (d) the corresponding geometric consistency parameter values for various noise levels. The green border in (b) and (c) has been drawn for illustrative purposes.

In the tables shown in Fig. 6(d) and Fig. 7(d) the results for the rectification of two representative InIms using arrays of square lenses are shown. For the artificial "Teapot" of Fig. 6 we can observe that the standard deviation of $\{\omega\}$ does not exceed 0.16° while the standard deviation of $\{\lambda\}$ does not exceed the value of 0.024 even for high noise contamination levels. These are typical results for the whole artificial InIm set, while we can further observe that the corresponding results for the optically acquired "Dice" of Fig. 7 are in line with the artificial simulation data.

Similarly in Fig. 8 and in Fig. 9 the rectification results for two characteristic InIms using arrays of circular lenses are shown. For the artificial "3D Objects" scene of Fig. 8 we can observe that the standard deviation of $\{\omega\}$ does not exceed the value of 0.87° while the standard deviation of $\{\lambda\}$ does not exceed the value of 0.041 even within high noise contamination levels. These results characterize the whole artificial InIm set, while it is further verified in Fig 9 and the corresponding table that the results for the optically acquired "Toy" are in line with the artificial InIm rectification data.

7 Conclusions

In this dissertation automated solutions were proposed to alleviate geometric distortions affecting the InIm acquisition process. The occurrence of this issue was studied over the whole range of available InIm configurations and effective solutions where proposed for its removal.

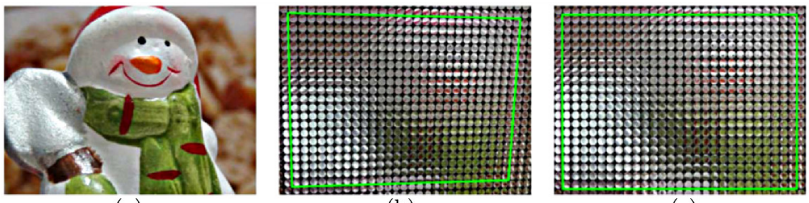

(a) (b) (c)

$\overline{\omega_i} + \sigma_{\omega_i}$	σ_{λ_i}
$90.00 \pm 0.46°$	0.039

(d)

Fig. 9. Rectification results for an optically acquired "Toy" InIm acquired using an array of circular lenses. (a) The original 2D image acquired for the "Toy", (b) the corresponding perspectively distorted InIm, (c) the rectified InIm, (d) the corresponding geometric consistency parameter values. The green border in (b) and (c) has been drawn for illustrative purposes.

The rectification of InIms acquired using square as well as hexagonal-triangular lenses was further optimized using a least squares approach while for the first time in current literature a novel and effective rectification methodology was proposed for arrays of circular lenses.

During the evaluation process, large sets of optically acquired as well as raytraced InIms were utilized to examine the parameters that may affect the robustness of proposed rectification frameworks. It should be noted that the usage of computationally generated InIm sets allowed joint control of both perspective distortion and noise levels.

The geometric consistency for the rectified InIms that are presented in this dissertation synopsis and the relevant publications [9–12] is fully retained as verified by the corresponding data. Since noise greatly affects the rectification procedure at the early processing stages, we conclude that the proposed methodologies are robust against high noise contamination levels and effective to to be used as an integrated and useful InIm analysis and rectification framework.

References

1. Lippmann, G.: La photographie integràle. Comptes-Rendus Academie des Sciences **146** (1908) 446–451
2. Son, J.Y., Javidi, B.: Three-dimensional imaging methods based on multiview images. J. Display Technol. **1**(1) (Sep 2005) 125
3. Park, J.H., Kim, Y., Kim, J., Min, S.W., Lee, B.: Three-dimensional display scheme based on integral imaging with three-dimensional information processing. Opt. Express **12**(24) (Nov 2004) 6020–6032
4. Jang, J.S., Javidi, B.: Formation of orthoscopic three-dimensional real images in direct pickup one-step integral imaging. Optical Engineering **42**(7) (2003) 1869–1870

5. Sgouros, N., Kontaxakis, I., Sangriotis, M.: Effect of different traversal schemes in integral image coding. Appl. Opt. **47**(19) (Jul 2008) D28–D37
6. Passalis, G., Sgouros, N., Athineos, S., Theoharis, T.: Enhanced reconstruction of three-dimensional shape and texture from integral photography images. Appl. Opt. **46**(22) (Aug 2007) 5311–5320
7. Sgouros, N.P., Athineos, S.S., Sangriotis, M.S., Papageorgas, P.G., Theofanous, N.G.: Accurate lattice extraction in integral images. Opt. Express **14**(22) (Oct 2006) 10403–10409
8. Hong, K., Hong, J., Jung, J.H., Park, J.H., Lee, B.: Rectification of elemental image set and extraction of lens lattice by projective image transformation in integral imaging. Opt. Express **18**(11) (May 2010) 12002–12016
9. Koufogiannis, E.T., Sgouros, N.P., Sangriotis, M.S.: Robust integral image rectification framework using perspective transformation supported by statistical line segment clustering. Appl. Opt. **50**(34) (Dec 2011) H265–H277
10. Koufogiannis, E.T., Sgouros, N.P., Sangriotis, M.S.: Perspective rectification of integral images produced using hexagonal lens arrays. In: Intelligent Information Hiding and Multimedia Signal Processing (IIH-MSP), 2012 Eighth International Conference on. (july 2012) 75–78
11. Koufogiannis, E., Sgouros, N., Ntasi, M., Sangriotis, M.: Grid reconstruction and skew angle estimation in integral images produced using circular microlenses. In: Digital Signal Processing (DSP), 2013 18th International Conference on, IEEE (2013) 1–7
12. Koufogiannis, E.T., Sgouros, N.P., Sangriotis, M.S.: Perspective rectification of integral images produced using arrays of circular lenses. Appl. Opt. **52**(20) (Jul 2013) 4959–4968
13. Lim, Y.T., Park, J.H., Kwon, K.C., Kim, N.: Resolution-enhanced integral imaging microscopy that uses lens array shifting. Opt. Express **17**(21) (Oct 2009) 19253–19263
14. Hartley, R.I., Zisserman, A.: Multiple View Geometry in Computer Vision. Second edn. Cambridge University Press (2004)
15. Liebowitz, D., Zisserman, A.: Metric rectification for perspective images of planes. In: Proceedings. 1998 IEEE Computer Society Conference on Computer Vision and Pattern Recognition (Cat. No.98CB36231), IEEE Comput. Soc (1998) 482–488
16. Kimme, C., Ballard, D., Sklansky, J.: Finding circles by an array of accumulators. Commun. ACM **18**(2) (February 1975) 120–122
17. Ip, H., Chen, Y.: Planar rectification by solving the intersection of two circles under 2d homography. Pattern Recognition **38**(7) (2005) 1117–1120
18. Lourakis, M.: Plane metric rectification from a single view of multiple coplanar circles. In: Proceedings - International Conference on Image Processing, ICIP. (2009) 509–512
19. von Gioi, R., Jakubowicz, J., Morel, J.M., Randall, G.: Lsd: A fast line segment detector with a false detection control. Pattern Analysis and Machine Intelligence, IEEE Transactions on **32**(4) (april 2010) 722–732
20. Theodoridis, S., Koutroumbas, K.: Pattern Recognition, Third Edition. 3 edn. Academic Press (2006)
21. Kovesi, P.: Matlab and octave functions for computer vision and image processing
22. Athineos, S.S., Sgouros, N.P., Papageorgas, P.G., Maroulis, D.E., Sangriotis, M.S., Theofanous, N.G.: Photorealistic integral photography using a ray-traced model of capturing optics. Journal of Electronic Imaging **15**(4) (2006) 043007